CHAPTER 3: RESULTS AND DISCUSSION

SYNTHESIS OF PALM OLEIC ACID-BASED MACROMERS

In view of the increasing interest in environmental protection, the use of vegetable oils in non-food applications has attracted appreciable attention. One of the specific areas is the use of vegetable oils for production of alkyd resins, which are extensively used in paints, adhesives [104], inks [105], varnishes [106] and various coatings. The properties of formulated alkyd resin, depends on the chemical composition and also their preparation processes. Various synthetic procedures, each with many variables, are used to produce different alkyd resins.

The use of vegetable oils such as linseed oil, soybean oil, castor oil and tall oil can impart to the alkyds certain properties, such as ability to air-dry, film hardness and durability and gloss retention, etc. Therefore, there is need to investigate native sources of oils for alkyd production.

Palm oil is classified as non-drying oil because of its low iodine value; alkyds made from palm oil are not capable of forming coherent film by air oxidation. Consequently, there are very little reports of the use of palm oil alone in the manufacturing of alkyds for coating application. Palm oil needs to mix with tung oil to produce a workable coating resin [84]. Another paper reported mixing the palm oil based-alkyds with melamine to form baking enamels [107].

This study describes the use of oleic acid, one of the palm oil derivatives, as raw material together with phthalic anhydride, PA, and glycerol to produce low molecular weight polyesters containing unsaturation (-C=C-) to function as macromers for copolymerization with MMA. For this project, three macromers were formulated with

different amounts of oleic acid, in combination with the other components to produce the macromers. The properties of the macromers were investigated with different characterization methods as will be mentioned in the next sections.

3.1 Synthesis of AlkOA65

AlkOA65 was prepared by polyesterification reaction from PA, oleic acid and glycerol. The AlkOA65 was formulated according to Patton's gel point calculation, which is an applicable alkyd formulation system to avoid gelation [99]. The theoretical calculation is demonstrated in Table 3.1.

Table 3.1 : Theoretical calculation for the formulation of macromer AlkOA65

Ingredient	**W(g)**	**E**	**e_A**	**e_B**	**F**	**m_0**
Glycerol	145	30.7	-	4.72	3	1.57
PA	103	74.0	1.39	-	2	0.70
Oleic acid	460	282.5	1.63	-	1	1.63
Total	708	-	3.02	4.72	-	3.90

where, W is weight of the raw material used; E is the equivalent weight (total of molecular mass divided by functionality); e_A is value of acid equivalent; e_B is value of hydroxyl equivalent; F is functionality and m_0 is total moles present at the beginning of reaction. The formulation of e_A, e_B and m_0 are represented as following:

$$e_A = \frac{W_{acid}}{E_{acid}} \qquad e_B = \frac{W_{hydroxyl\ \ compound}}{E_{hydroxyl\ \ compound}} \qquad m_0 = \frac{e_A}{F} \text{ or } \frac{e_B}{F}$$

Patton's gel point (constant K) refers to the extent of reaction when gelation might occur [99]. K is defined as in the following formula and should be greater than 1.00, so that gelation would not occur at 100% reaction conversion.

$$\text{Patton's gel point constant K} = \frac{\sum m_0}{\sum e_A}$$

If the Patton gel point constant is 0.90 then gelation might occur at 90% conversion. From Table 3.1, the K for AlkOA65 was 1.29 and gelation will not happen at 100% of reaction. The excess of hydroxyl groups in AlkOA65 could be estimated by taking the ratio between e_A and e_B, as in the following formula:

$$\text{Excess of hydroxyl group} = \frac{\sum e_B}{\sum e_A} = 1.56$$

This points out that in the macromer formulation there is 56% of excess –OH groups. From Table 3.1, AlkOA65 was formulated as a long oil length macromer with (100×460)/ 708, i.e., 65 parts oleic acid per 100 g resin.

According to the references [108, 109], the amount of polyhydric alcohol used in the formulation of alkyd resin varies between 5 to 40% by weight. If the amount of polyhydric alcohol is greater than 40% by weight, the unreacted polyhydric alcohols in the alkyd system will show an excessive increase in absorption moisture. Furthermore, if the polyhydric alcohol content is less than 5% by weight, the molecular weight of the finished alkyd resin is difficult to improve. While for polybasic acids, the desirable content varies from 10 to 50% by weight.

The excess amount of polybasic acid of more than 50% by weight may cause increase in side reactions during synthesis which will take into account for the gel formation at high temperature. Furthermore, extra amount of polybasic acid can have effect on tackiness of the finished alkyd, resulting in alkyd resin with low tackiness.

On the other hand, if polybasic acid content is less than 10%, polycondensation reaction will hardly progress. As displayed in Table 3.1, the glycerol and PA contents in AlkOA65 are (100 ×145/708), i.e. 20.5 and (100 ×103/708), i.e. 14.5% respectively, thus these ratios are in the desirable range in an alkyd formulation.

Average functionality (F_{av}) is also an important factor which reflects the overall ability of the macromer in crosslinking. Average functionality is defined as following formula:

$$F_{av} = \frac{e_A + e_B}{m_0} = 1.98$$

3.2 Synthesis of AlkOA40

AlkOA40 was synthesized with the same procedure as with AlkOA65. The theoretical formulation is summarized in Table 3.2.

Table 3.2 : Formulation of AlkOA40

Ingredient	**W(g)**	**E**	**e_A**	**e_B**	**F**	**m_0**
Glycerol	256	30.7	-	8.34	3	2.78
PA	338	74.0	4.57	-	2	2.29
Oleic acid	400	282.5	1.42	-	1	1.42
Total	994	-	5.99	8.34	-	6.49

3.3 Synthesis of AlkOA28

AlkOA28 was prepared in the same manner as with other macromers. The theoretical calculation is shown in Table 3.3. According to Table 3.3, F_{av} for AlkOA28 is 2.3.

Table 3.3 : Formulation of AlkOA28

Ingredient	W(g)	E	e_A	e_B	F	m_0
Glycerol	456	30.7	-	14.85	3	4.95
PA	700	74.0	9.46	-	2	4.73
Oleic acid	452	282.5	1.6	-	1	1.6
Total	1608	-	11.06	14.85	-	11.28

3.4 Reduction of the acid number during the preparation of macromer

Progress of the polycondensation reaction, during the synthesis of macromers was monitored by periodically checking the acid number of the reaction mixture.

A typical titration results for acid number determination for AlkOA65 for 440 minutes is shown in Table 3.4 and Table 3.5, respectively.

Table 3.4 : Titration results for standardization of alcoholic KOH

Determination	First determination	Second determination
KHP (g)	0.5001	0.4985
Alcoholic KOH required (mL)	47.2	46.6
Normality	0.052	0.052
Average Normality	0.052	

where, Normality was determined based on the equation [2.1] in Section 2.2.2, Chapter 2.

Table 3.5 : Titration results of AlkOA65 with standardized alcoholic KOH at 440 min

Determination	First trial	Second trial
Weight of AlkOA65 (g)	3.2246	3.2083
Alcoholic KOH required for titration of the blank, V_b (mL)	0.3	0.3
Alcoholic KOH required for titration of the sample, V (mL)	9.31	9.25
Acid number (mg KOH /g resin)	8.151	8.138
Average acid number (mg KOH /g resin)	8.14	

where, acid number was calculated based on the equation [2.2] in Section 2.2.3, Chapter 2. The values of determined acid numbers and $\overline{X}_n$ throughout the synthesis of macromers are tabulated in Table 3.6, Table 3.7 and Table 3.8 for synthesis AlkOA65, AlkOA40 and AlkOA28 respectively. $\overline{X}_n$ was calculated using equation 3.2 and 3.3 (Section 3.4.1).

Table 3.6 : Variation of acid number with reaction time and $\overline{X}_n$ during the synthesis of AlkOA65

Reaction time (min)	**Acid number(mg KOH/g resin)**	$\overline{X}_n$
0*	239.3	-
60	175.4	1.4
130	86.00	2.8
190	33.7	7.1
205	28.5	8.4
220	23.0	10.4
235	19.7	12.2
250	17.6	13.5
266	15.7	15.2
280	14.5	16.4
295	13.5	17.9
310	12.2	19.6
325	10.9	21.7
340	10.0	23.8
365	9.7	24.4
380	9.4	25.6
395	8.9	27.0
411	8.6	27.8
426	8.4	28.6
440	8.1	29.4

* refers to initial acid number are calculated using following formula:

$$\text{Initial acid number} = \frac{56100 \times e_A(\text{Total})}{\sum W} \qquad [3.1]$$

Table 3.7 : Variation of acid number and $\overline{X}_n$ during the synthesis of AlkOA40

Reaction time (min)	Acid number (mg KOH/g resin)	$\overline{X}_n$
0*	338.1	-
60	125.8	2.7
90	93.1	3.6
120	74.4	4.5
159	55.7	6.1
192	46.3	7.3
242	30.0	11.2
292	24.5	13.9
344	21.0	16.1
394	18.0	18.9
447	15.6	21.7
501	12.3	27.8
551	10.6	32.3
611	8.9	38.5

Table 3.8 : Variation of acid number and $\overline{X}_n$ during the synthesis of AlkOA28

Reaction time (min)	Acid number (mg KOH/g resin)	$\overline{X}_n$
0*	385.9	-
50	170.0	2.3
90	139.1	2.8
130	112.0	3.4
170	94.4	4.1
210	87.2	4.4
250	67.0	5.7
290	60.7	6.4
340	48.0	8.1
390	39.0	9.9
440	30.5	12.7
500	26.1	14.7
550	25.6	15.2
600	22.8	16.9
650	21.6	17.9
700	18.6	20.8
750	18.4	20.8
800	16.0	24.4

Changes in the acid number with increasing reaction time for the different macromers are plotted in Figure 3.1. As can be observed, the decrease in acid number is faster in the early stages than the later stages during the reaction time for all samples. These changes in acid number have been elucidated on the basis of the different reactivity of primary and secondary OH groups of glycerol.

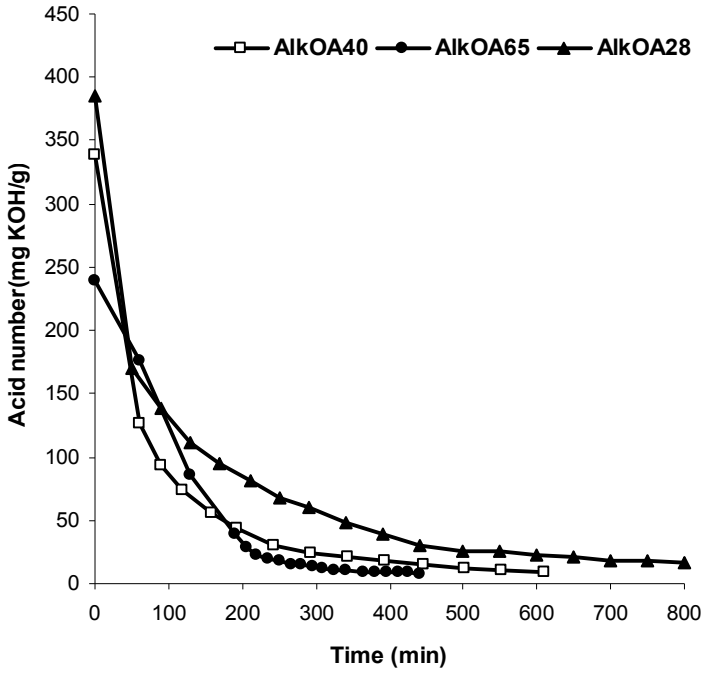

Figure 3.1 : plots of changes in acid number versus reaction time for macromers

Figure 3.2 shows a plausible reaction mechanism in the preparation of macromers. Since primary OH group is more reactive than secondary OH group, indeed rapid decrease in acid number at the initial stages of reaction occurs when primary hydroxyl groups react followed by secondary OH groups react in the later stages [110].

It has been also stated that reduction in acid number in later stages could be related to the formation of crosslinks or branching between the chains [111] and consequently increases viscosity in the reaction medium.

With reference to Figure 3.1, the least rapid decrease in acid number is observed for for AlkOA65. Above 50 min, 60 min and 130 min of reaction time for AlkOA28, AlkOA40 and AlkOA65 alkyds respectively, the plots show gradual decrease in acid number for three samples. Therefore, the ratio of glycerol to acid in the alkyd formulation can influence on the rate of reduction acid number.

Aigbodion and Okieimen also obtained similar results [112] where the rate of change in acid number for alkyd resin with 50% and 34% oil content were higher than that of alkyd resin having 60% oil.

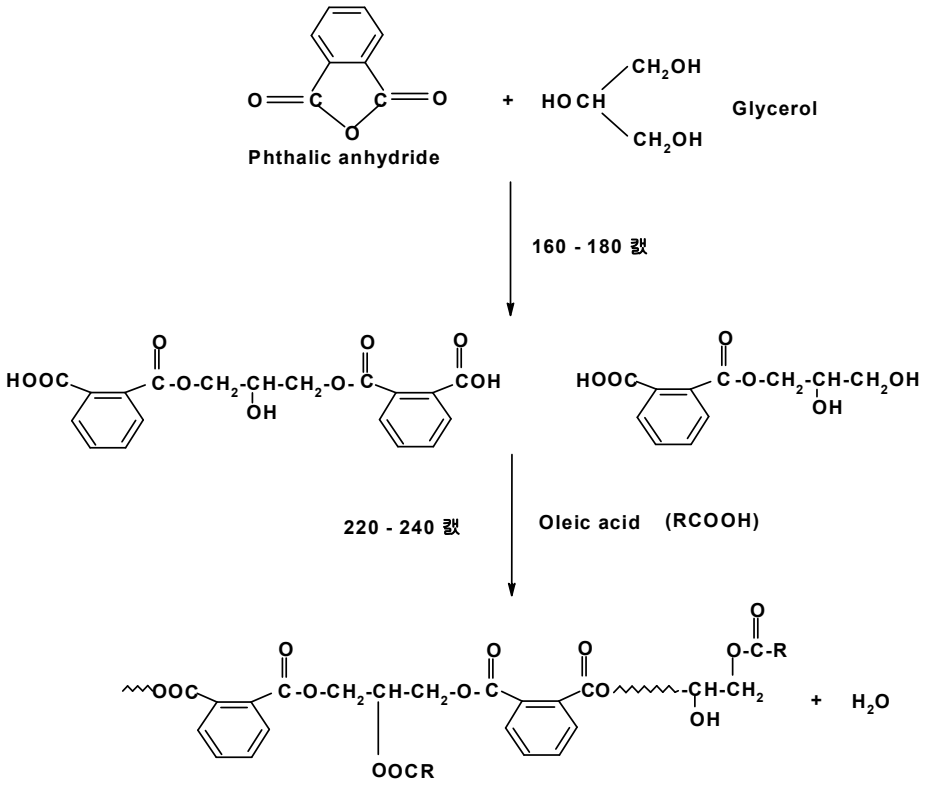

Figure 3.2 : A plausible reaction mechanism in the polyesterification of the macromers where R stands for CH_3-$(CH_2)_7$-CH=CH-$(CH_2)_7$-

According to the Figure 3.2, in the preparation of the macromers, the reaction of PA involved two distinct steps. As, PA is much more reactive than oleic acid, thus the first step

of reaction with most of the primary OH groups of glycerol proceeds rapidly by ring opening of the anhydride ring to form a half ester and a free carboxylic group. This step did not evolve any water and occurred quite readily around 160-180°C. As the reactions are depicted in Figure 3.2, when the temperature was increased to 220-240°C, the carboxylic acid group of the half ester and oleic acid would compete to react with the remaining hydroxyl groups in the mixture and the water of condensation was collected in the Dean-stark decanter.

3.4.1 Calculation of extent of reaction and average degree of polymerization based on acid number:

The extent of reaction, P, was calculated from end group analysis of aliquots of the reaction mixture withdrawn at various time intervals during the reaction using the following equation [3.2].

$$P = [(AN_0 - (AN)_t]/(AN)_0 \qquad [3.2]$$

Where:

$(AN)_0$ = Acid number at the zero time

$(AN)_t$ = Acid number at the distinct time

The average degree of polymerization, $\overline{X}_n$ defined as the average number of structural units per polymer chain, was calculated based on P using equation [3.3] at different times of reaction.

$$\overline{X}_n = (1 - P)^{-1} \qquad [3.3]$$

Tables of 3.6, 3.7 and 3.8 display the average degree of polymerization for AlkOA65, AlkOA40 and AlkOA28 respectively. As has been reported earlier [113], poly-

functional and mono-functional polyesterification reactions can be expressed as a second-order rate law. Equation [3.4] shows the rate law expression.

$$(1 - P)^{-1} = C_0 kt + 1 \qquad [3.4]$$

where k is the rate constant, while t refers to reaction time and C_0 is initial concentration of the reactants i.e. acid number. Corresponding to the equation [3.4], graphs of $(1\text{-}P)^{-1}$ against time of reaction should be linear if k is constant during the reaction time. Figure 3.3 shows that the graphs for the three macromers during the first stage are linear up to certain limit whereby straight-line plots are obtained and after 190-210 min the graphs deviate from linearity.

The first linear part is considered to represent time of formation of linear molecules due to existence of higher content of glycerol and PA in the formulation of the samples at the initial portion while the second part (non linear part) depicts period of formation of complex branching or crosslinking in the macromer chains. Aigbodion and Okieimen, and also Satheesh et al. reported similar trend for alkyds modified with rubber seed oil [114], African locustbean seed oil [112] and Jatropha oil [111] in the synthesis of alkyd resins respectively. Table 3.9 shows the extent of reaction and the average degree of polymerization calculated at the deviated point from linearity for all the three samples.

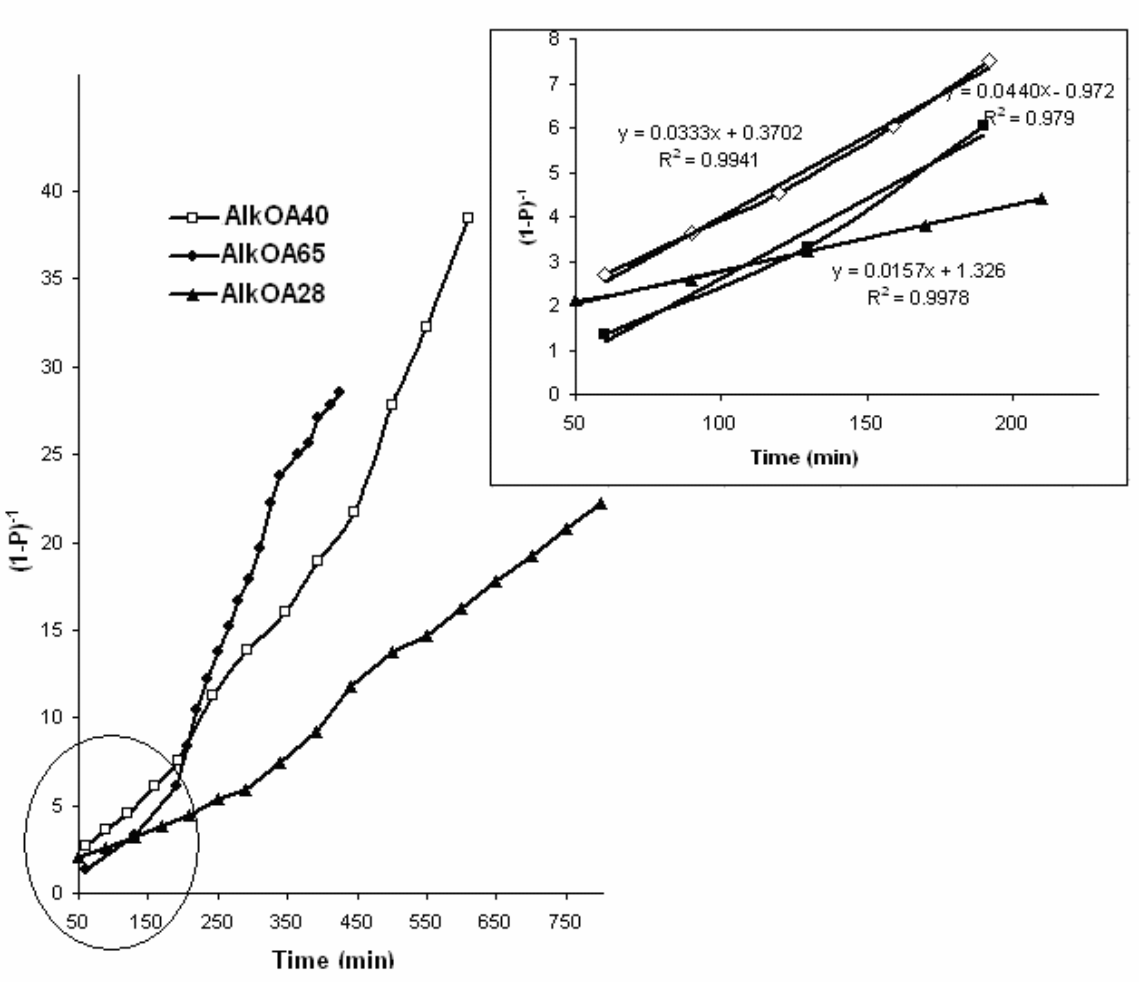

Figure 3.3 : Graphs of $(1- P)^{-1}$ against time for the macromer samples

Table 3.9 : Calculated P%, $\overline{X}_n$ and *k* at the deviate point from linearity, and P% at the end of reaction for the macromers

Macromers	Kinetic parameters				
	Time (min)	P%	$\overline{X}_n$	$k \times 10^5$ g $(mgKOH)^{-1}$ min^{-1}	P% at the end of reaction
AlkOA28	210	77.4	4.4	4.1	95.9
AlkOA40	192	86.3	7.3	9.8	97.4
AlkOA65	190	85.9	7.1	18	96.6

The results reveal that the extent of reaction at these regions changes 77.4 to 85.9%. In accordance to the results obtained for reaction between PA and glycerol which varied between 75-80%, the results obtained from palm oleic acid based macromers indicate a significant degree of conversion [115]. The results obtained from palm oleic acid based-macromers also show significant extent of reaction at the end of reaction as exhibited in Table 3.9.

The second-order rate constants, *k*, calculated through the linear part of Figure 3.3 are tabulated in Table 3.9. Sample AlkOA65 shows the largest value of 18×10^{-5} g (mg KOH)$^{-1}$ min^{-1}. These results prove that ratio of the reactants used (PA, glycerol and oleic acid) in the reaction affects the polyesterification rate. The smallest *k* and P% was obtained for AlkOA28 which can be attributed to the relatively highest molecular weight and consequently highest viscosity.

As the mixture became more viscous after reaching a certain conversion level, the molecular chains motion would become very slow even at the end of reaction. As such, AlkOA28 shows the least extent of the reaction and rate constant.

3.5 Characterization of synthesized macromers

In this section, concentrations of carboxylic and hydroxyl groups were determined from titration method. FTIR and ^{1}H-NMR spectroscopies as common techniques are then used to identify and confirm the functional groups present in the chemical structures of the resulting macromers. In addition, the functional groups in the macromers are compared to the oleic acid functional groups. ^{13}C-NMR spectroscopy is used to recognize configuration of -C=C- in macromers. Thermal stability is studied using DSC and TGA. From TGA

results activation energy and thermal degradation mechanism of the macromers were also investigated.

3.5.1 Hydroxyl number determination of macromers

Determination of hydroxyl number of macromer was accomplished in two stages; in the first stage free hydroxyl groups in the macromer was esterified with PA, subsequently in the second stage hydroxyl number was measured from the amount of unreacted PA remained which was neutralized by NaOH. In hydroxyl number calculation, before the titration, sample size of the macromer must be calculated by substituting the estimated hydroxyl number using equation [3.5] into equation [2.4] as shown in Section 2.2.6.

$$\text{Estimated hydroxyl number} = \frac{(\sum e_B - \sum e_A) \times 56100}{\sum W - \text{Water evolved}} \qquad [3.5]$$

where water evolved is $[e_A\ (PA) \times 9] + [e_A\ (\text{oleic acid}) \times 18]$.

Therefore, according to the Table 3.1 and equations 3.5, estimated hydroxyl number for AlkOA65 was calculated as following:

$$\text{Estimated hydroxyl number} = \frac{(4.72 - 3.02) \times 56100}{708 - (1.39 \times 9 + 1.63 \times 18)} = 143.17$$

Corresponding to the equation [2.4] in Chapter 2, sample size for this macromer was (561÷ 143.17), i.e. 3.92 g.

Hydroxyl number is determined by the standard test method (Chapter 2, Section 2.2.6), involving reacting the hydroxyl compound with excess phthalic anhydride, and then back titrate for the remaining acid. An example of titration results for the standardization of NaOH solution and hydroxyl number of AlkOA65 were shown in Table 3.10 and Table 3.11 respectively.

Table 3.10 : Standardization of NaOH solution

Determination	**First trial**	**Second trial**
Weight of potassium hydrogen phthalate/g	4.4878	4.4622
NaOH solution required /mL	44.4	44.1
Normality	0.4950	0.4955
Average Normality/ N	0.495	

★ where normality was calculated using the equation [2.3] in section 2.2.5., Chapter 2.

Table 3.11 : Titration results of AlkOA65 with standardized NaOH solution

Determination	**First trial**	**Second trial**
Sample size/ g	3.9205	3.9198
NaOH solution required for titration of the blank /mL	95.1	95.0
NaOH solution required for titration of the sample /mL	75.2	75.2
Hydroxyl number (mg NaOH/ g sample)	140.95	140.27
Average hydroxyl number (mg NaOH/ g sample)	140.6	
Estimated hydroxyl number	143.2	

★ where, hydroxyl number was calculated using the equation [2.5] in Section 2.2.6, Chapter 2.

The titration results for AlkOA40 and AlkOA28 are tabulated in Tables 3.12 and 3.13 respectively.

Table 3.12 : Titration results of AlkOA40 with standardized NaOH solution

Determination	**First trial**	**Second trial**
Sample size/ g	3.9321	3.9289
NaOH solution required for titration of the blank /mL	95.1	95.2
NaOH solution required for titration of the sample /mL	75.9	75.8
Hydroxyl number (mg NaOH/ g sample)	135.6	137.1
Average hydroxyl number (mg NaOH/ g sample)	136.4	
Estimated hydroxyl number	142.2	

Table 3.13 : Titration results of AlkOA28 with standardized NaOH solution

Determination	First trial	Second trial
Sample size/ g	3.9321	3.9501
NaOH solution required for titration of the blank /mL	95.0	95.1
NaOH solution required for titration of the sample /mL	76.1	76.4
Hydroxyl number (mg NaOH/ g sample)	133.5	131.5
Average hydroxyl number (mg NaOH/ g sample)	132.5	
Expected hydroxyl number	142.3	

Table 3.14 represents the hydroxyl numbers, acid numbers and estimation of the properties for three macromers as stated from the titration method.

Table 3.14 : Hydroxyl and acid numbers of macromers

Property	Macromer		
	AlkOA65	AlkOA40	AlkOA28
Hydroxyl number (mg NaOH / g sample)	140.6	136.4	132.5
Acid number (mg KOH/ g sample)	8.1	8.9	16
-OH concentration*/ mol g^{-1}	2.5×10^{-3}	2.4×10^{-3}	2.4×10^{-3}
-COOH concentration*/ mol g^{-1}	1.4×10^{-4}	1.6×10^{-4}	2.9×10^{-4}
Ratio of –OH/ -COOH	17.9	15	8.3

* where,

$$\text{-OH concentration} = \frac{\text{Hydroxyl number}}{56100}, \qquad \text{–COOH concentration} = \frac{\text{Acid number}}{56100}$$

From Table 3.14, ratios of –OH to –COOH, demonstrate all macromers were perpetually formulated with excess hydroxyl groups.

3.5.2 FTIR spectroscopy

Figure 3.4 indicates the overlaid FTIR spectra of macromers and oleic acid while, the assignments of major absorption peaks for these spectra are tabulated in Table 3.15.

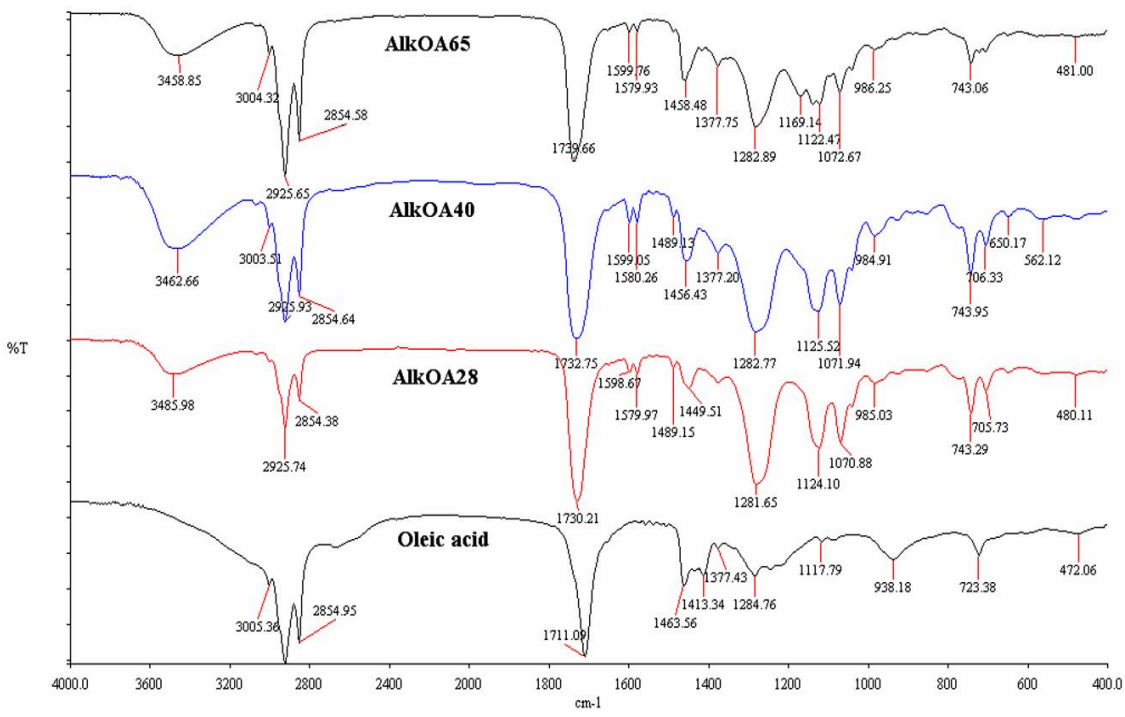

Figure 3.4 : Infrared spectra of the AlkOA macromers and oleic acid

The characteristic bands are observed at 1730-1740 cm^{-1} for ester group and twin peaks at 1580 to 1599 cm^{-1} shows C=C stretching conjugated skeletal ring breathing modes of the aromatic group from PA. The broad OH stretching bands at 3458-3486 cm^{-1} confirm the presence of free hydroxyl groups which are observable in all the macromers except for oleic acid. Bands are observed at 1450-1458 cm^{-1} for C-H bending of CH_2, 1281-1283 cm^{-1} and 1070-1125 cm^{-1} for C-O-C stretching of ester; all these bands support the structure of macromers formed as suggested in the reaction.

Table 3.15 : Major absorption peaks of macromers in FTIR spectra

Bonding	Wave number/cm^{-1}
OH stretching	3458-3486
C-H stretching aromatic and aliphatic	2925, 2854
C=O stretching carbonyl groups	1730- 1740
C=C stretching aromatic rings(PA)	1580, 1599
C-H bending of CH_2	1450-1458
Aromatic =C-H bending	744
C-O-C stretching of ester groups	1070-1283

3.5.3 ^{1}H-NMR spectroscopy

The structure of the macromers was further confirmed by ^{1}H-NMR spectroscopy. Figure 3.5 shows the ^{1}H-NMR spectrum of the AlkOA40 together with molecular structure of the macromer. The peaks at chemical shifts δ 7.4 -7.8 ppm are due to the aromatic proton of phthalic ester (j). The peaks (h,i) at 5.3 ppm are attributed to the vinylic protons –CH=CH- of the oleic acid, while the terminal $–CH_3$ in the chain end of the oleic acid (a) is at 0.89 ppm. The primary (f) and secondary protons (g) on the glycerol unit appear as a very broad peak at 3.6-4.7 ppm (lower field) due to the electronegativity of oxygen. The sharp resonance (b) at 1.3 ppm was attributed to the secondary protons of $–CH_2$ of the oleic acid; while the allylic protons of $–CH_2$ in fatty acid structure appeare as a weaker resonance (c) at 2.1 ppm. The CH_2 protons (e) on the oleic acid unit are deshieled due to electronegativity of adjacent carboxylic group to the CH_2 protons and appear around 2.3 ppm. The strong peak at 7.26 ppm is assigned to the $CDCl_3$ solvent.

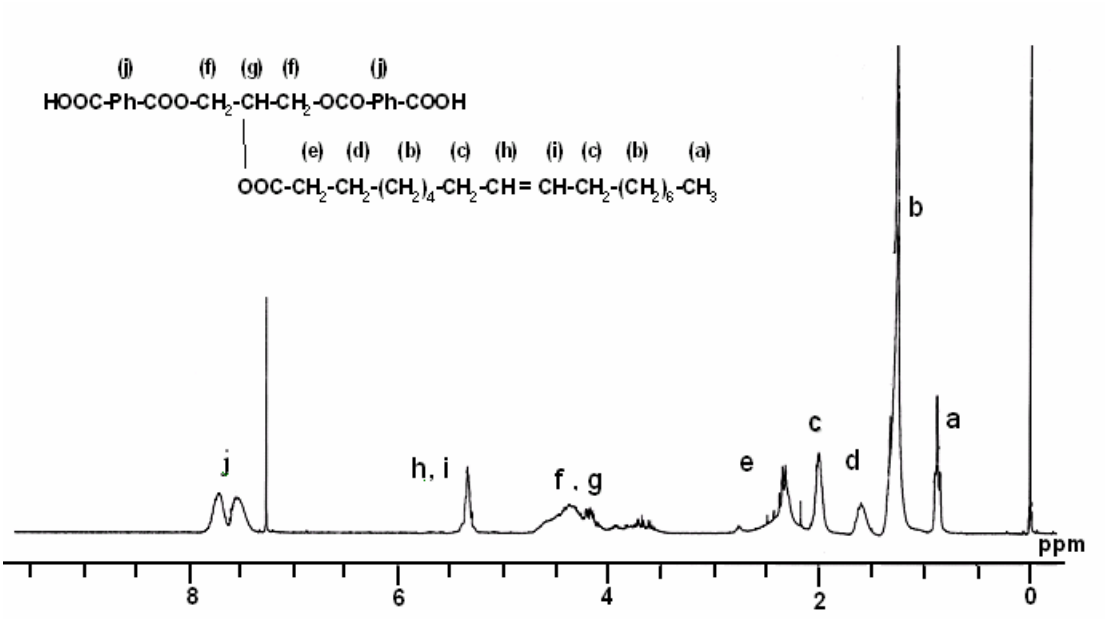

Figure 3.5 : ^{1}H-NMR spectrum and one of the plausible molecular structures of AlkOA40

The ratio of integrations of peaks at 5.3 ppm to 0.89 ppm is 0.67, in agreement with the oleic acid structure in the macromer. ^{1}H-NMR spectra of AlkOA65 and AlkOA28 are shown in Appendix A.

3.5.4 ^{13}C-NMR Spectroscopy

Natural oleic acid occurs in the cis-configuration at the -C=C-. Comparing the ^{13}C-NMR spectra of oleic acid and macromer in Figures 3.6 (a) and (b) revealed that the oleic acid moiety in the macromer still maintained the cis-configuration at the -C=C- as shown by the peaks 129.6-129.9 ppm. The assignments of the various carbons arising from oleic acid and macromer are shown in Table 3.16. The peak at 77 ppm is assigned to the $CDCl_3$ solvent.

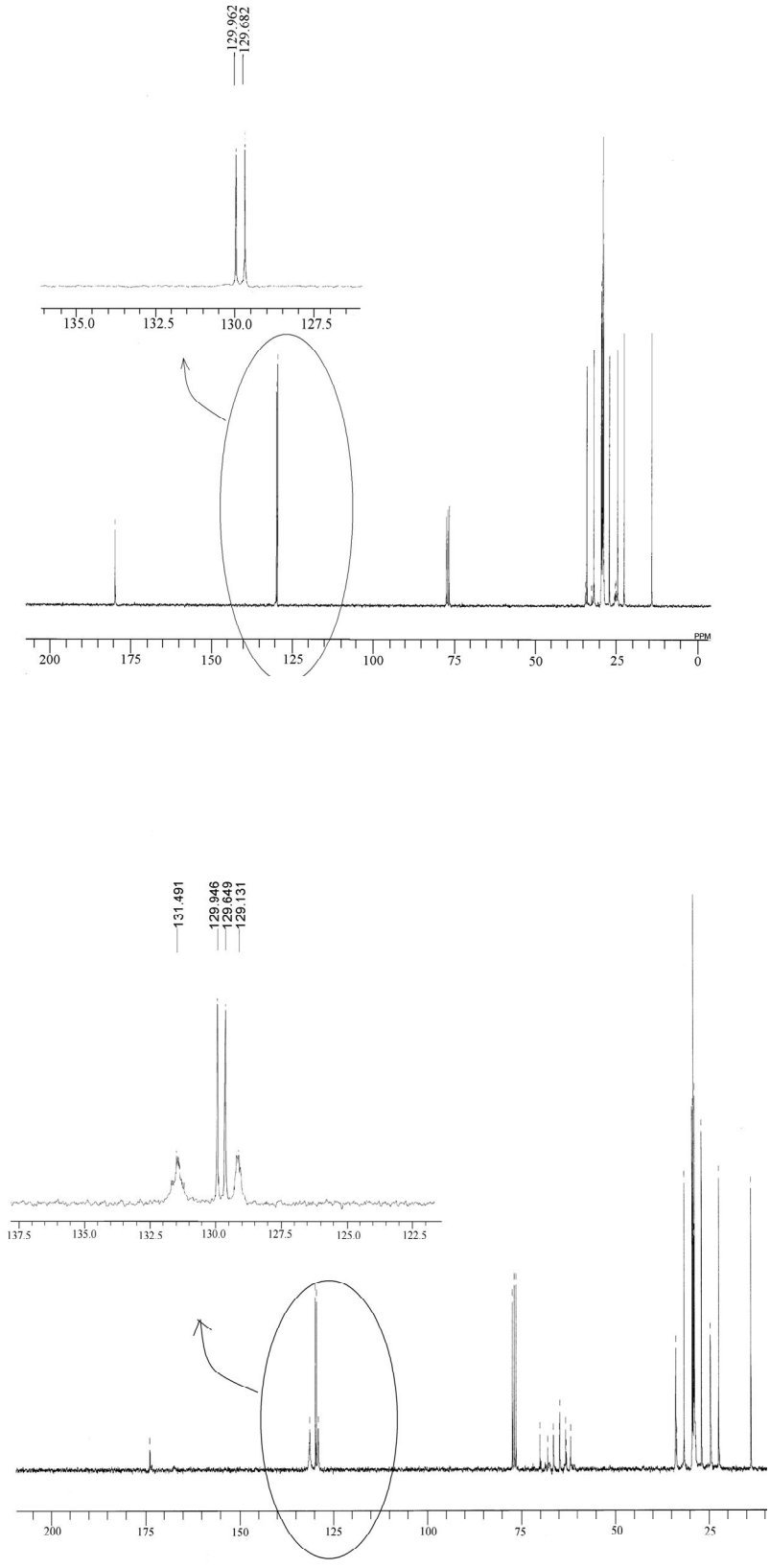

Figure 3.6 : ^{13}C-NMR Spectra for oleic acid (a) and macromer AlkOA65 (b)

Table 3.16 : Chemical shifts of ^{13}C-NMR spectra of oleic acid and macromer

Chemical shift (δ)/ ppm	Assignment
14 (protons of methyl groups)	**CH_3**-$(CH_2)_7$-CH=CH-
22.5-34.5	Different kinds of **(-CH_2-)** groups in oleate branches
60-70.1	-O-**CH_2**-**CH**(O)-**CH_2**(O)- in glycerol moiety
129.6- 129.9	–**CH=CH**- (Aliphatic) from oleate branches
129.1- 131.4	–**CH=CH**- (Aromatic ring)
170-185	**C=O** (Arising from ester and acid groups)

3.5.5 Gel-permeation chromatography (GPC)

The number average molecular weight (M_n), weight average molecular weight (M_w) and polydispersity index of the macromers were determined by GPC. The molecular weight characteristics of macromers are shown in Table 3.17. Whereby, the M_n as well as M_w of the macromers increases with increasing of PA and decreasing of oleic acid in the macromers. AlkOA28 macromer shows the highest molecular weight and broadest distribution.

Table 3.17: The molecular weight characteristics of macromers

Macromer code	PA (%)	(M_n)	(M_w)	(M_w/M_n)
AlkOA65	14.5	907	1829	2.0
AlkOA40	34.0	1285	3311	2.6
AlkOA28	43.5	2018	10479	5.2

3.5.6 Differential Scanning Calorimetry (DSC analysis)

One of the most important basic characteristic of a polymer is its glass transition temperature. The glass transition temperature of the macromer samples with different oil

lengths were measured using DSC. The T_g of the macromers vary between -36˚C to -39˚C as shown in Table 3.18. DSC thermograms of macromers were represented in Appendix B.

Table 3.18: Glass transition temperatures of macromers

Macromer code	**$T_g \pm 2$/˚C**
AlkOA65	-36.80
AlkOA 40	-38.86
AlkOA28	-39.08

3.5.7 Thermogravimetric analysis (TGA)

TGA is an important technique that provides valuable information on thermal stability of polymer. Thermal degradation of the three macromers was studied by determining their mass loss during heating at programmed heating rate under nitrogen atmosphere. Overlay of TG and DTG curves at heating rate of 10˚C min^{-1} for the three macromers are presented in Figures 3.7a and 3.7b respectively. From these thermograms, it can be seen that AlkOA28 has relatively higher thermal stability followed by AlkOA40 and AlkOA65.

In the TG curves, only one single stage mass loss was observed. To investigate the relative thermal stability, T_d (-2.5 wt.%), at which 2.5 wt.% of original macromer has already been thermally degraded and lost, was empirically taken as an index to compare its thermal stability. This temperature, T_d, as shown in Figure 3.7b is 271˚C for alkOA28 and 200˚C and 190˚C for AlkOA40 and AlkOA65 respectively.

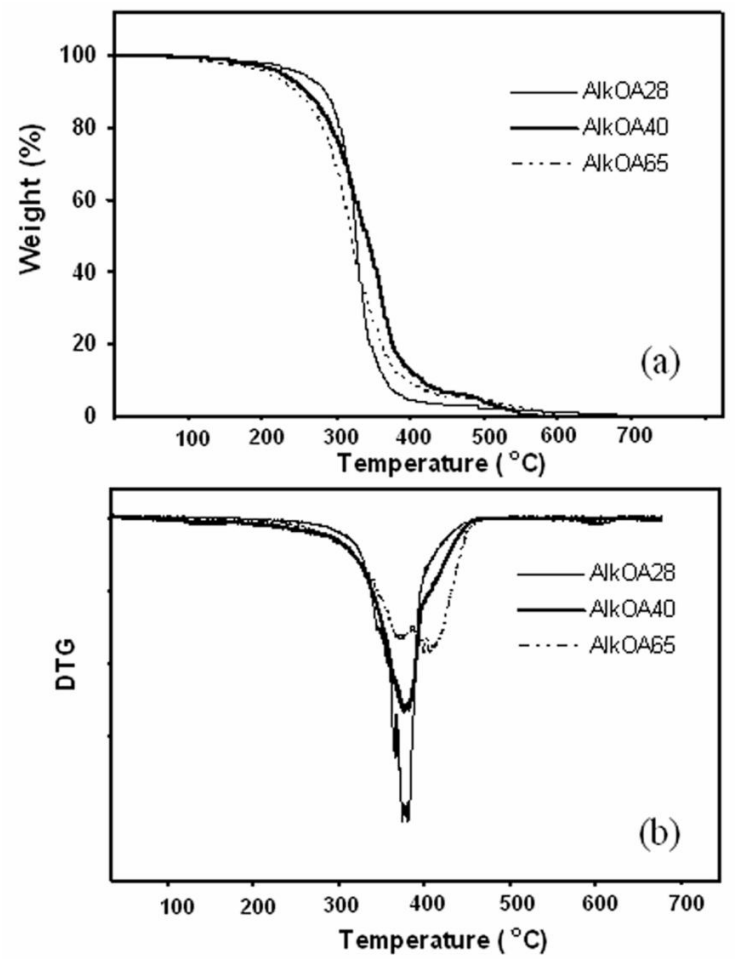

Figure 3.7 : TG (a) and DTG (b) curves of three macromers at heating rate 10°C/min

These early stages of the decomposition and such a pre-major weight loss may be due to volatilization of small molecules in the polymer [116].

3.5.7.1 Activation energy using Kissinger equation

The kinetic parameters of the polymers can provide important additional information for their use and process ability as new materials. In order to understand and predict the performance of macromers versus temperature, it is necessary to obtain the kinetic parameters. Non-isothermal methods have been used extensively for the determination of

kinetic parameters. To further analyze the degradation mechanisms of the macromers it is important that the kinetic parameters, activation energy E_d, pre-exponential factor A and degradation rate constant, *k*, be evaluated.

Looking at TG and DTG curves of AlkOA28 at different heating rates (Figure 3.8), it is clear that the peak temperature, T_p, which is the temperature at maximum rate of decomposition where peak deflection occurs in the DTG curves, shifts to higher values with increasing heating rate.

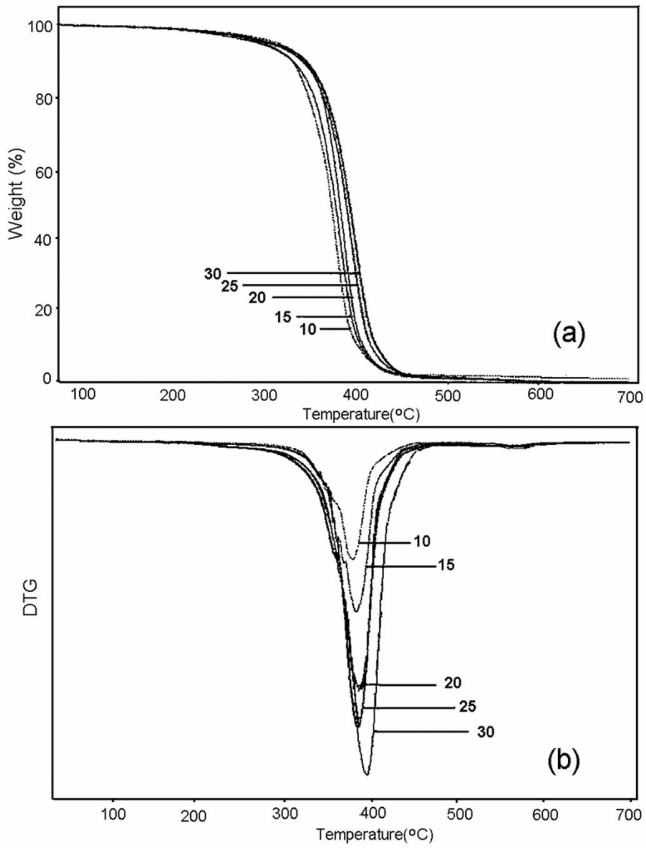

Figure 3.8 : TG (a) and DTG (b) thermograms of AlkOA28 at various heating rates

Similar results are observed for both AlkOA40 and AlkOA65 using its DTG thermograms (Figure 3.9b and 3.10b) where an increment of 17˚C for AlkOA28, 20˚C for AlkOA40 and 26˚C for AlkOA65 are obtained (Table 3.19).

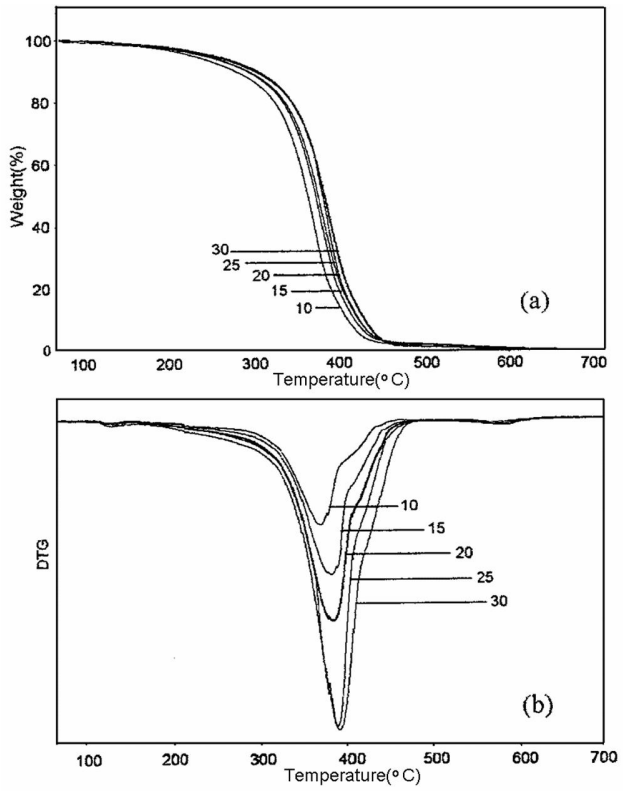

Figure 3.9 : TG (a) and DTG (b) thermograms of AlkOA40 at various heating rates

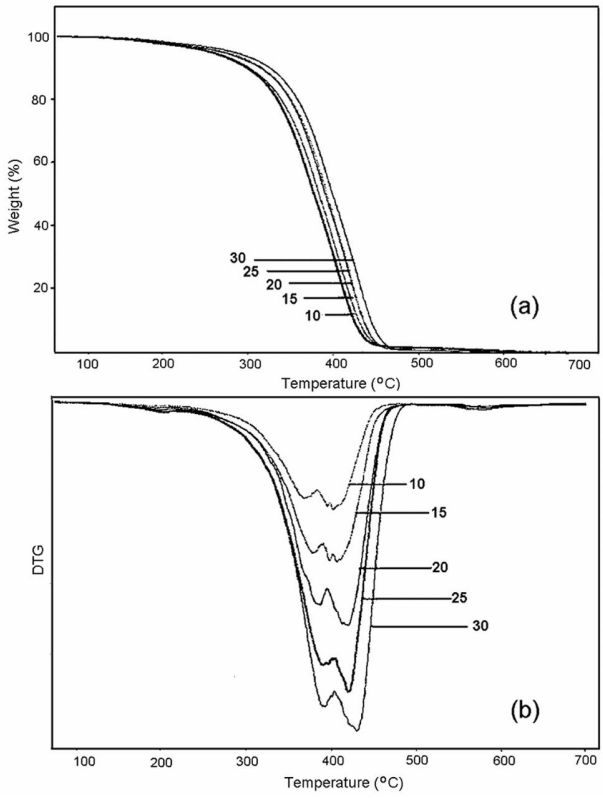

Figure 3.10 : TG (a) and DTG (b) thermograms of AlkOA65 at various heating rates

Table 3.19: E_d, A and *k* at different heating rates using Kissinger plots

Macromer	q ($K\ min^{-1}$)	T_p (K)	A (s^{-1})	E_d ($kJ\ mol^{-1}$)	Average A (s^{-1})	*k* (s^{-1})	Average (*k*)
AlkOA28	10	649.44	2.78×10^{16}	229.0	2.98×10^{16}	0.011	0.021
	15	653.9	3.08×10^{16}			0.016	
	20	658.35	3.04×10^{16}			0.021	
	25	660.41	3.32×10^{16}			0.026	
	30	666.28	2.71×10^{16}			0.031	
AlkOA40	10	644.98	5.88×10^{12}	183.0	5.72×10^{12}	0.009	0.017
	15	653.35	5.55×10^{12}			0.013	
	20	658.05	5.73×10^{12}			0.017	
	25	662.76	5.57×10^{12}			0.021	
	30	665.11	5.9×10^{12}			0.025	
AlkOA65	10	674.59	1.4×10^{8}	134.0	1.61×10^{8}	0.006	0.011
	15	677.29	1.89×10^{8}			0.009	
	20	690.66	1.53×10^{8}			0.011	
	25	695.11	1.63×10^{8}			0.014	
	30	700.68	1.6×10^{8}			0.016	

The activation energy of decomposition can be estimated via the Kissinger equation [3.6] [117].

$$-\ln\left(\frac{q}{T_p^{\,2}}\right) = \frac{E_d}{RT_p} - \ln\left(\frac{AR}{E_d}\right) \qquad [3.6]$$

where q is the heating rate, T_p, as it noted earlier, is the temperature at maximum rate of decomposition where peak deflection occur in the DTG curves, R is the gas constant, A is the pre-exponential factor and E_d is the decomposition activation energy. The plots of $-\ln(q/T_{p2})$ against $1/T_p$ for three samples are shown in Figure 3.11.

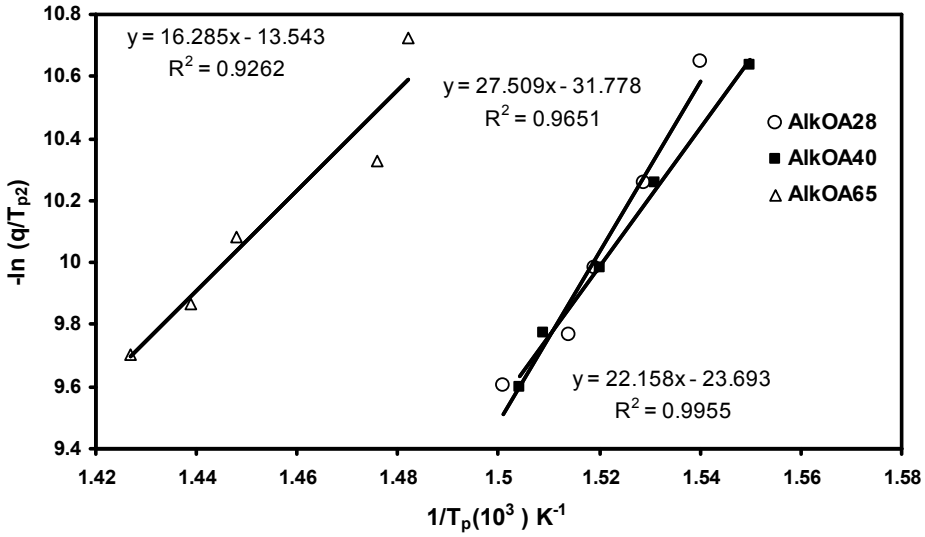

Figure 3.11 : Determination of E_d by Kissinger method for the three macromers

Thermal decomposition activation energies (E_d) were calculated from the slopes of the straight lines of $-\ln (q/T_p^2)$ versus $1/T_p$. The results are shown in Table 3.19.

In the following part, kinetic parameters were calculated for AlkOA28 as an example.

Equation for linear curve in Figure 3.11: $y = 27526\ x - 31.805$

With gradient E_d/R in equation [4.6] = 27526(K)

$$E_d = 27526 \times 8.3143$$

$$E_d = 228859.4218\ (J\ mol^{-1})$$

$$E_d = 228.86\ (kJ\ mol^{-1})$$

From the equation [3.6] $A = \dfrac{q \times E_d}{R \times T_p^2} \exp^{(\frac{E_d}{R} \times \frac{1}{T_p})}$

When $q = 10\ K\ min^{-1}$, $T_p = 649.44\ (K)$

$$A_{10} = \frac{10 \times 228859.4218 \times \exp(\frac{228859.4218}{8.3143})(\frac{1}{649.44})}{8.3143 \times (649.44)^2}$$

$= 1.66684 \times 10^{18}\ (min^{-1}) = 2.78 \times 10^{16}\ (s^{-1})$

When q = 15 K min^{-1}, T_p = 653.9 (K)

$A_{15} = 1.8471 \times 10^{18}\ (min^{-1}) = 3.08 \times 10^{16}\ (s^{-1})$

When q = 20 K min^{-1}, T_p = 658.35(K)

$A_{20} = 1.82796 \times 10^{18}\ (min^{-1}) = 3.04 \times 10^{16}\ (s^{-1})$

When q = 25 K min^{-1}, T_p = 660.41(K)

$A_{25} = 1.99307 \times 10^{18}\ (min^{-1}) = 3.32 \times 10^{16}\ (s^{-1})$

When q = 30 K min^{-1}, T_p = 666.28 (K)

$A_{30} = 1.62758 \times 10^{18}\ (min^{-1}) = 2.71 \times 10^{16}\ (s^{-1})$

Average (A_{10}:A_{30}) = $2.99 \times 10^{16}\ (s^{-1})$

From the calculated activation energies in Table 3.19, an improvement in the thermal stability of the samples can be seen with an increase in the PA and glycerol. AlkOA28 shows relatively the highest thermal stability due to the highest activation energy followed by AlkOA40 and AlkOA65. The trend in thermal stability of the macromers may also be due to enhancement of the intermolecular attraction among the polymer chains. The increasing number of –OH groups in the macromer formulation and the formation of hydrogen bonds between –OH groups in glycerol may have effect on increasing the thermal stability. The improved thermal stability can also be explained through the reduced mobility of the polymer chains in the polyesters. PA can usually hinder the motion of the

polymer chains. During thermal decomposition of samples, relatively weak bonds break at lower temperature whereas the stronger bonds in the aromatic rings take place at higher temperature [118, 119]. The oleic acid, due to its long chain is more thermally labile and thus decreases the thermal stability. It is well known that differences in the molecular weights may also affect the thermal degradation behaviour of polymers [120]. The balance of all these reasons has significant contribution to the increment of the thermal stability of AlkOA28.

Using the Arrhenius equation [3.7] below, the degradation rate constant, k, at T_p, calculated are as shown in Table 3.19 whereby increasing the heating rate, the degradation rate constants shift to higher values.

$$k = A.\exp^{\frac{-E_d}{RT_p}} \qquad [3.7]$$

Using AlkOA28 as an example, the kinetic parameter, k, was calculated at heating rate 10˚C min^{-1}.

At heating rate of 10 K min^{-1} T_p = 649.44 (K)

$k = 2.78 \times 10^{16} \exp^{-228859.4218 / (8.3143 \times 649.44)}$

$k = 0.011$ (s^{-1})

3.5.7.2 Activation energy and thermal degradation mechanism of the macromers using isoconversional method of Ozawa, Flynn and Wall (OFW)

Ozawa, Flynn and Wall equation [3.8] [121, 122] was used to clarify relationship between activation energy and degree of conversion (α) in the decomposition reactions. This method includes the measuring of the temperatures corresponding to fixed values of α from experiments at different heating rates (q).

$$\ln(q) = \ln\left[\frac{A f(\alpha)}{d\alpha / dT}\right] - \frac{E_d}{RT} \qquad [3.8]$$

The graph, ln q versus 1/T is used to construct the Ozawa plot, where q is the heating rate, T is the temperature from the various heating rates at the same loss weight, E_d the activation energy and R the gas constant.

The OFW method is a method which assumes that conversion function f (α) does not change with the alteration of the heating rate for all values of α. If the determined activation energy, E_d, is the same for the various values of α, the existence of a single–step reaction can be concluded with confidence. On the contrary, a change of E_d with increasing degree of conversion is an indication of a complex reaction mechanism that invalidates the separation of variables involved in the OFW analysis [123]. The following section describes the OFW analysis of the three samples.

3.5.7.3 Kinetic analysis of AlkOA28 degradation using OFW method

Firstly, the Ozawa method was used to calculate the activation energy for different conversion values by fitting the plots of ln (q) against 1/T. Some of the Ozawa plots for AlkOA28 which has the largest M_n, 2018 are displayed in Figure 3.12 and all data are summarized in Table 3.20. (See Appendix N for calculations)

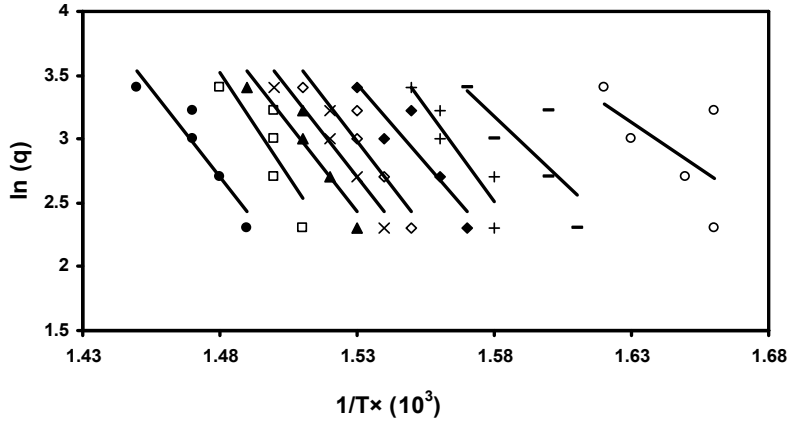

Figure 3.12 : Ozawa plots of AlkOA28 at various conversion of reaction: α = 0.1(○), α = 0.2 (-), α = 0.3 (+), α = 0.4 (♦), α = 0.5 (◊), α = 0.6 (×), α = 0.7 (▲), α = 0.8 (□), α = 0.9 (•)

Table 3.20 : Calculated E_d using the Ozawa method at various conversion using different heating rates for the three macromers

Conversion (α)	E_d (kJ mol^{-1})		
	AlkOA28	**AlkOA40**	**AlkOA65**
0.1	109.6	107	105.8
0.2	168.3	151.3	141.5
0.3	243.9	165.4	169
0.4	247.9	176.6	177.3
0.5	247.5	187.1	191.5
0.6	252.6	195.6	192.7
0.7	254.4	208.6	194.8
0.8	284.1	209.2	219.8
0.9	302.1	243.6	224.4

It is clear from DTG thermograms of AlkOA28 (Figure 3.8b), the mass loss follows at least two stages under all heating rates. These stages are: first in the temperature region close to 376 to 390˚C and second step is before 700˚C. Therefore, for the precise kinetic description of mass loss, at least two different mechanisms have to be considered. However in OFW method, the equation used is derived assuming constant activation energy,

introducing systematic error in the estimation of E_d [124]. Thus, the dependence of E_d on α value, as calculated with OFW method, can be separated in three distinct regions corresponding to the different degradation processes of sample during heating (Figure 3.13); the first for values of α up to 0.3, (I) in which E_d presents an important increase, the second ($0.3 < \alpha < 0.7$) in which E_d presents no increase (II) and in third region for $0.7 < \alpha < 0.9$ in which E shows again a significant increase (III). This dependence of E_d on α is an indication of a reaction with the participation of at least three different mechanisms and each one mechanism presents different activation energy.

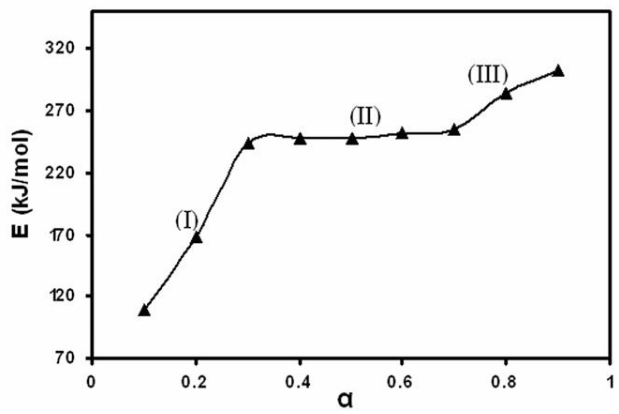

Figure 3.13 : Activation energies corresponding to fixed values of α using Ozawa plots of AlkOA28

3.5.7.4 Kinetic analysis of AlkOA40 degradation using OFW method

The thermogravimetric curves of AlkOA40 having M_n = 1285 g mol^{-1} at different heating rates were shown in Figure 3.9. With reference to the DTG thermograms of AlkOA40 (Figure 3.9b), the mass loss follows 3 stages but these stages are indistinguishable in the TG curves. These 3 stages are: first in the temperature region close to the 130˚C, second between 371 to 392˚C and the third is before 700˚C. Hence, to enable detailed kinetic description of mass loss, at least three different mechanisms have to be

considered. The activation energy of degradation of the studied macromer as estimated using this method also corresponds to distinct values of α during the reaction. Some of the Ozawa plots for AlkOA40 between 10% and 90% weight loss are displayed in Figure 3.14 and as mentioned before data are summarized in Table 3.20. (See Appendix N for calculations)

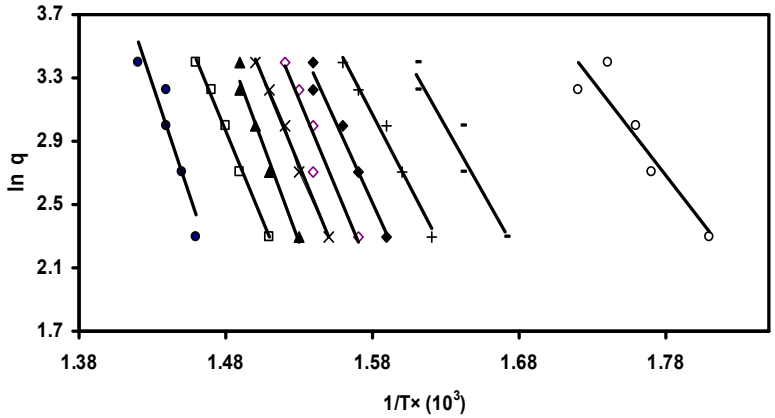

Figure 3.14 : Ozawa plots of AlkOA40 at various conversion of reaction: α = 0.1(○), α = 0.2 (-), α = 0.3 (+), α = 0.4 (♦), α = 0.5 (◊), α = 0.6 (×), α = 0.7 (▲), α = 0.8 (□), α = 0.9 (•)

The results as shown in Figure 3.15 reveal that the dependence of E_d on α value calculated according to the different degradation processes can be divided by four distinct regions.

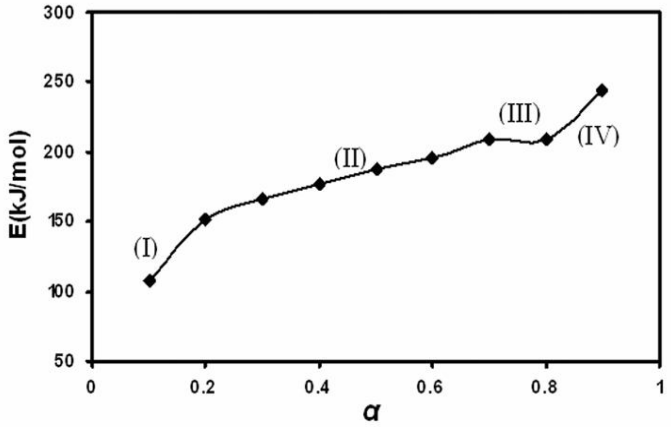

Figure 3.15 : Activation energies corresponding to fixed values of α using Ozawa plots of AlkOA40

The first one is for values of α up to 0.2, in which E_d presents a significant increase, the second for values between $0.2 < \alpha < 0.7$ in which E_d shows a slight monotonous increase, the third region appears between $0.7 < \alpha < 0.8$ in which E_d shows no increase and the fourth region can be seen for $\alpha > 0.8$ whereby E_d displays an important increase. This dependence of E_d on α is an indication of a complex reaction comprising of at least four different mechanisms. The activation energies for this sample are very small at the initial stages of decomposition and higher at the final stages. These initial lower values are most likely associated with initiation process that occurs at weak links of the polymer. By increasing the temperature, random scission of macromolecular chains predominates.

3.5.7.5 Kinetic analysis of AlkOA65 degradation using OFW method

The thermogravimetric curves of AlkOA65 with M_n= 907 g mol^{-1} at different heating rates are shown in Figure 3.10. From the DTG thermograms of AlkOA65 (Figure 3.10b); it can be seen that the mass loss occurs in a minimum 4 of stages under all heating rates. These stages are obvious: first in the region of the between 100 to 200˚C, second around 368˚C and the third step is between 400 to 428˚C and final stage takes place before 700˚C. Therefore, for the exact kinetic description of mass loss, at least four different mechanisms have to be taken into account. Figure 3.16 shows Ozawa plots for AlkOA65 between 10 to 90% weight loss at different heating rates. (See Appendix N for calculations) Figure 3.17 shows that the dependence of E_d on α values that were calculated using OFW method.

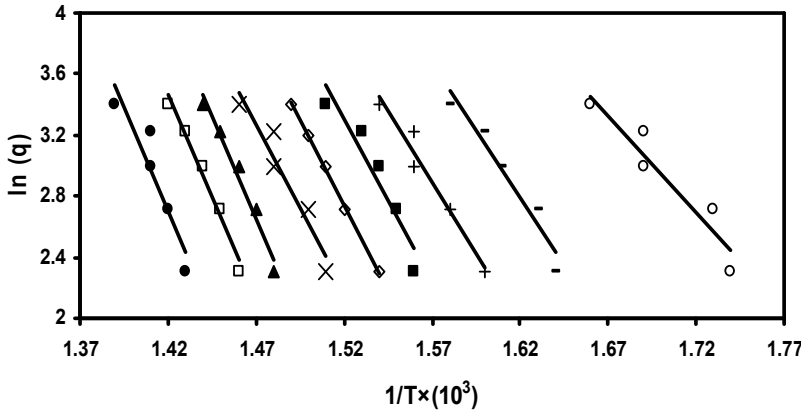

Figure 3.16 : Ozawa plots of AlkOA65 at various conversion of reaction: α = 0.1(○), α = 0.2 (-), α = 0.3 (+), α = 0.4 (♦), α = 0.5 (◊), α = 0.6 (×), α = 0.7 (▲), α = 0.8 (□), α = 0.9 (•)

From the slopes of the Figure 3.17, the degradation process can be separated in five regions for this sample. The initial stage of decomposition that occurs up to $\alpha < 0.3$ shows an important increase in activation energy, the second stage appears at $0.3 < \alpha < 0.5$ in which E_d demonstrates a small increment, the third region at $0.5 < \alpha < 0.7$ displays no increase in activation energy, the fourth stage of decomposition appears at $0.7 < \alpha < 0.8$ presents a big increase in activation energy and the final region for $\alpha > 0.8$ in which E_d exhibits a slight increase again.

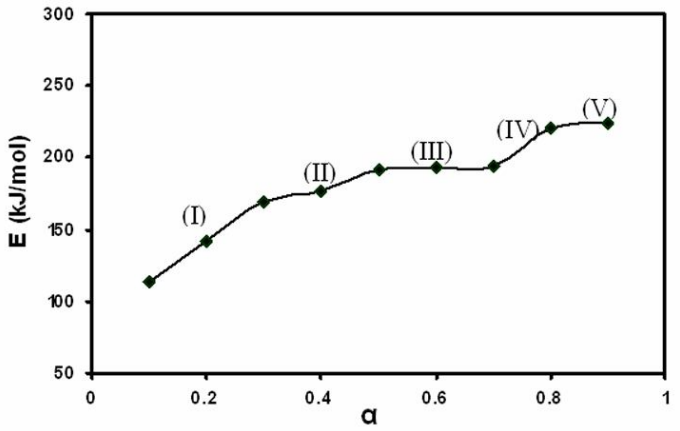

Figure 3.17 : Activation energies corresponding to fixed values of α using Ozawa plots of AlkOA65

This dependence of E_d on α indicates a complex reaction and also proves the effect of molecular weight of the alkyds on reaction mechanism. By using OFW method, decreasing the molecular weight of macromer reveals more complexity in degradation reaction and all results are consistent with the presence of overlapped peaks in the DTG curves.

3.6 Summary

Three macromers with different percentage of oleic acid, phthalic anhydride and glycerol were synthesized. From Kissinger method, the activation energies of thermal degradation for the macromers AlkOA28, AlkOA40 and AlkOA65 are found to be 229.0, 183.0 and 134.0 kJ mol^{-1} respectively. Using the Arrhenius equation, the average degradation rate constant, k, at T_p, calculated for AlkOA28, AlkOA40 and AlkOA65 are 0.021, 0.017 and 0.011.

Ozawa, Flynn and Wall (OFW) method was used to clarify relationship between activation energy and degree of conversion (α) in decomposition reactions. From OFW method, the dependence of activation energy on the α value for AlkOA28, was recognized by the existence of three regions for E_d values and that of AlkOA40 was indicated by four regions, while for AlkOA65 the existence of five regions for E_d values was identified. In addition, the OFW method reveals more complexity in the degradation reactions with decrease in the molecular weight of the macromers. The thermal properties of the macromers improve as the PA/oleic acid ratio is increased from 0.22 in AlkOA65 to 1.55 in AlkOA28 and glycerol/oleic acid ratio raised up from 0.32 in AlkOA65 to 1 in AlkOA28. The oleic acid, due to its long chain is more thermally labile and thus decreases the thermal stability.